



Published in final edited form as:

*Neuron*. 2008 November 26; 60(4): 555–569. doi:10.1016/j.neuron.2008.09.011.

## Distinct Stages of Myelination Regulated by $\gamma$ -Secretase and Astrocytes in a Rapidly Myelinating CNS Coculture System

Trent A. Watkins<sup>\*</sup>, Ben Emery, Sara Mulinyawe, and Ben A. Barres

Stanford University School of Medicine, Department of Neurobiology, Fairchild Science Building D235, Stanford, California 94305-5125

### SUMMARY

Mechanistic studies of CNS myelination have been hindered by the lack of a rapidly myelinating culture system. Here we describe a versatile CNS coculture method that allows time-lapse microscopy and molecular analysis of distinct stages of myelination. Employing a culture architecture of reaggregated neurons fosters extension of dense beds of axons from purified retinal ganglion cells. Seeding of oligodendrocyte precursor cells on these axons results in differentiation and ensheathment in as few as three days, with generation of compact myelin within six days. This technique enabled: (1) demonstration that oligodendrocytes initiate new myelin segments only during a brief window early in their differentiation, (2) identification of a contribution of astrocytes to the rate of myelin wrapping, and (3) molecular dissection of the role of oligodendrocyte  $\gamma$ -secretase activity in controlling the ensheathment of axons. These insights illustrate the value of this defined system for investigating multiple aspects of CNS myelination.

### INTRODUCTION

The extension of myelin sheaths by oligodendrocytes (OLs) is critical for the rapid conduction of electrical signals in the CNS, as evidenced by the severe loss of function associated with multiple sclerosis (MS) and other demyelinating disorders. Understanding the molecular signals that control multiple stages of OL and myelin development is needed to devise strategies for promoting myelin repair. Established techniques, such as the culture of purified oligodendrocyte precursor cells (OPCs), have enabled extensive characterization of the events leading to OL generation, including proliferation, migration, and differentiation. In contrast, current methods have been inadequate for elucidating the molecular basis of OL myelination, the multi-step process of adhesion to axons, ensheathment, wrapping, and compaction. Although several myelinating culture systems have been developed, each method has significant limitations that restrict its mechanistic utility. A rapidly myelinating simplified system that permits independent manipulation of defined populations of CNS neurons and glia

<sup>\*</sup>Present Address (To whom correspondence should be addressed): Trent A. Watkins Division of Research Genentech Inc., 1 DNA Way, South San Francisco, CA 94080 Tel: (650) 467-5276 e-mail: trentw@gene.com.

#### SIGNIFICANCE

The regulation and mechanisms of CNS myelination are poorly understood, reflecting the paucity of tools available for molecular dissection. This study describes the development of a rapid, versatile, and defined *in vitro* model of myelination that can be used to elucidate the cellular and molecular mechanisms underlying multiple stages of CNS myelination. This system enables investigation of axonal ensheathment by oligodendrocyte processes, demonstrating both regulation by oligodendrocyte  $\gamma$ -secretase and a brief window for myelination during early oligodendrocyte development. Astrocytes, in contrast, specifically promote later stages of myelin wrapping. These insights provide tools and ideas for studies of myelin repair.

**Publisher's Disclaimer:** This is a PDF file of an unedited manuscript that has been accepted for publication. As a service to our customers we are providing this early version of the manuscript. The manuscript will undergo copyediting, typesetting, and review of the resulting proof before it is published in its final citable form. Please note that during the production process errors may be discovered which could affect the content, and all legal disclaimers that apply to the journal pertain.

would serve as a valuable tool for dissecting the axonal regulation and molecular mechanisms of myelination.

Broadly, CNS myelinating culture systems can be divided into three classes: (1) slice cultures, (2) mixed cultures, and (3) cocultures of purified cells. In perinatal cerebellar slice cultures, endogenous axons are myelinated over a period of 2–4 weeks (Notterpek et al., 1993). Mixed cultures consist of crude assortments of dissociated cells from a particular region of the embryonic CNS, such as the forebrain, cerebellum, or spinal cord, maintained for weeks until OLs develop from endogenous progenitors (Lubetzki et al., 1993; Svenningsen et al., 2003; Thomson et al., 2006). Although slice and mixed cultures may benefit from the inclusion of all cell types found *in vivo*, their complexity and the challenges of targeting specific cells for genetic manipulation undermine many of the advantages provided by *in vitro* approaches.

Cocultures of purified neurons and glia offer a means of studying myelination in a more defined system. Cocultures of Schwann cells with TrkA<sup>+</sup> neurons of the dorsal root ganglia (DRGs) are used for a wide range of studies (Bunge, 1987). Cocultures of these neurons with OPCs also results in myelination, particularly when NGF is neutralized (Chan et al., 2004). These cocultures, while useful for some studies, have limitations for understanding myelination of CNS axons. First, DRGs are not CNS neurons, and the mechanisms of central and peripheral myelination differ in some essential features. Secondly, their axons extend only a short distance into the spinal cord and remain largely unmyelinated, hindering the design of complementary *in vivo* experiments. Thirdly, these cocultures can take an extraordinary time to develop, with three weeks of DRG culture followed by one week of proliferation of OPCs before the appearance of OLs. Finally, the mitogenic response of OPCs to DRG axons precludes effective transient transfection and the assessment of individual OLs. To better understand the mechanisms of myelination, there is a considerable need for a more rapid CNS coculture system.

The optic nerve has long served as a model system for *in vivo* studies of CNS myelination, making it an attractive target for developing a complementary *in vitro* system. Importantly, retinal ganglion cells (RGCs), whose axons make up the optic nerve, are among the few CNS neurons for which there are established protocols for purification and culture (Meyer-Franke et al., 1995). Despite these properties, early cocultures of dissociated RGCs and OPCs failed to generate myelin, even in the presence of astrocytes (Meyer-Franke et al., 1999). Here we use clusters of reaggregated RGCs to facilitate growth of dense beds of axons, leading to substantial myelination. This rapid coculture system enables a variety of studies to dissect intrinsic and extrinsic controls of OL maturation. Using this technique, we have performed genetic manipulations to gain insights into the regulation of axonal ensheathment, time-lapse microscopy to observe intrinsic changes in the capacity to myelinate as an OL matures, and cocultures with purified white matter astrocytes to evaluate their contribution to myelin growth.

## RESULTS

### Establishment of a Myelinating CNS Coculture System

Given the limitations of current *in vitro* models for dissecting the molecular mechanisms of CNS myelination, we aimed to develop a rapidly myelinating system that allows for genetic analysis and for expanded flexibility of cell sources. We began with standard procedures for isolating perinatal rat RGCs and promoting neurite outgrowth *in vitro* in the absence of glial support (Meyer-Franke et al., 1995). Incubation on  $\alpha$ -Thy1-coated Petri dishes (*i.e.*, immunopanning) selects RGCs from suspensions of dissociated retinal cells (see Supplemental Material). These purified neurons, when cultured on laminin-coated glass coverslips in a serum-free medium containing B27 supplement, extend a network of neurites (Figure S1A). Established serial immunopanning protocols are then used to isolate perinatal rat cells

expressing the OPC marker A2B5 but not the OL marker galactocerebroside (GC) from suspensions of dissociated optic nerve cells (Barres et al., 1994). These purified OPCs serve as a source for the generation of OLs in coculture with RGCs. We initially found, however, that the networks of neurites extended by dissociated RGCs *in vitro* are not conducive to ensheathment of axons by OL processes (Figures S1A and S1B). We have therefore developed an alternative culture architecture that uses reagggregates of purified RGCs to generate dense beds of axons that serve as a more reliable substrate for myelination (Figure S1A).

Figure 1A illustrates the resulting OPC-RGC reaggregate coculture system. Culture of purified rat or mouse RGCs at high density results in reagggregates that extend dense beds of axons after plating on laminin-coated coverslips. OPCs are then purified from developing cortex or optic nerves from either rats or mice. These OPCs may be plated directly onto RGC reaggregate cultures or transfected by nucleofection or adenoviral vectors prior to seeding. The resulting coculture consists of a bed of axons dotted with developing OL-lineage cells (Figure 1B). When sparsely plated, the cell fates and morphologies can be assessed with little ambiguity by immunostaining for markers of OPCs (NG2), OLs (myelin basic protein, MBP), and astrocytes (glial fibrillary acidic protein, GFAP) (Figure 1B). Thus two stages of OL development important for myelination can be assessed by immunolabeling OL-lineage markers, **differentiation** of OPCs to OLs, and **ensheathment** of axons, distinguished morphologically from simple membrane extension by the formation of smooth tubes of MBP<sup>+</sup> membrane (Figure 1C). The subsequent stage, the **wrapping** of axons to generate multiple layers of compact myelin, can be assessed by electron microscopy (EM) or the use of lipophilic dyes (such as Sudan Black) that preferentially label the multiple layers of lipid-rich membrane characteristic of mature myelin. This system has enabled us to explore myelination by OL-lineage cells from a variety of sources (species, anatomical region, and stage of development), and to evaluate the contributions of different CNS cells and molecules to each of the three stages of myelin development.

### Enhancement of Differentiation and Ensheathment by $\gamma$ -Secretase Inhibitors

Using this reaggregate architecture, six days of coculture between rat RGCs and optic nerve OPCs resulted in examples of OLs that extended multiple distinctive tubes of MBP<sup>+</sup> membrane around axons (Figure S1B). The new coculture arrangement, however, did not ensure that every OPC would develop into a myelinating OL. Instead, most of the OPCs were inhibited from differentiating or diverted to an astrocyte fate by coculture with RGCs (Figures 1B and 2C), and the majority of MBP-expressing OLs still failed to clearly ensheath axons (Figures S1B and 3B). Thus the coculture of reagggregates with OPCs enables myelination, but RGC axons under these conditions do not optimally promote differentiation and ensheathment.

We explored means of increasing the numbers of OPCs that develop into myelinating OLs. Previous work demonstrated that Notch1 signaling inhibits the differentiation of OPCs and that RGC axons in culture express the Notch ligand Jagged1 (Wang et al., 1998). To test whether Notch1 is responsible for the failure of differentiation, we treated cocultures over six days with DAPT (1  $\mu$ M), an inhibitor of  $\gamma$ -secretase, a protease required for Notch1 activation (De Strooper et al., 1999; Dovey et al., 2001). The addition of DAPT enhanced both differentiation and myelination, with significant increases in both MBP<sup>+</sup> OLs (Figure 2C) and the proportion of those OLs that ensheathed axons to generate multiple smooth MBP<sup>+</sup> tubes (Figure 3B). In the presence of DAPT, ensheathment could be observed within three days of coculture (Figure 2A), with a number of myelinating OLs visible by day four (Figure 2B). By the sixth day of coculture, greater than 70% of the OPCs in axon-dense regions had become myelinating OLs (Figure 2C). These results are consistent with the proposed role for Notch1 activation in controlling differentiation and raise the possibility that  $\gamma$ -secretase might also be

involved in regulating the ensheathment of axons. The pharmacological inhibition of  $\gamma$ -secretase therefore provides a simple means to achieve rapid myelination in this system.

### Adaption of Coculture Method to Cortical OPCs

The small numbers of OPCs available from optic nerves prompted us to adapt the coculture for use with cortical OPCs. Purification from one or two rat brains typically generated enough OPCs for a number of different analyses. We began by examining whether  $\gamma$ -secretase inhibitors promote differentiation and myelination in cortical OPC cocultures. DAPT promoted cortical OL differentiation, but to a lesser degree than was observed with optic nerve cells (Figure 3A). This suggests that differentiation of both cortical and optic nerve OPCs is inhibited by  $\gamma$ -secretase-mediated signals (*e.g.*, Notch1), and that cortical OPCs are also affected by DAPT-insensitive cues. Despite this difference, DAPT equivalently increased the proportions of cortical and optic nerve OLs that ensheathed axons, suggesting that this enhancement of myelination is not simply a consequence of increased differentiation (Figure 3B).

We next evaluated the time course of a number of myelin markers in a medium formulation (MyM) that more reliably supports wrapping and compaction (Supplemental Material). We found that the myelin proteins CNPase, MBP, and, to a lesser extent, proteolipid protein (PLP), were expressed as early as the third day of coculture in the presence of DAPT (Figures 3C and 3F). At this early time point, we also found isolated examples of OLs expressing the late marker myelin-oligodendrocyte glycoprotein (MOG) and ensheathing axons (Figures 3D and 3F). To assess whether this expression and morphology correlated with the deposition of multiple layers of myelin membrane, we labeled cocultures with the lipophilic dyes Sudan Black or Fluoromyelin Red. This analysis revealed faint myelin segments as early as day 5, with conspicuous staining seen one week after seeding of OPCs (Figures 3E–3G). The presence of compact myelin at day 7 was confirmed by EM (Figure 3H). Over twelve days, myelinating OLs induced clustering of axonal proteins into structures resembling nodes of Ranvier (Figure 3I). Together, these data validate the use of acutely-isolated, purified cortical OPCs to study myelination of RGC axons in culture.

### Use of Mouse RGCs and Optic Nerve OPCs in Myelinating Cocultures

In order to facilitate the use of existing genetic tools, we next adapted the system for mouse neurons and OPCs. We developed an immunopanning protocol for purifying OPCs from mouse optic nerves, and established cocultures of these cells with mouse RGCs, purified using a slight modification to the rat protocol (Supplemental Material). Interestingly, these mouse cocultures differed in some respects from similar rat cocultures. Unlike rat optic nerve OPCs (and similar to cortical OPCs),  $\gamma$ -secretase inhibition did not substantially disinhibit differentiation, with the majority of mouse OPCs remaining NG2<sup>+</sup> or becoming astrocytes (Figures 4A and 4C). Nonetheless, DAPT enhanced myelination, such that more than half of the OLs ensheathed axons over six days (Figure 4E). These results establish the use of mouse RGCs and optic nerve OPCs in this coculture system.

Given the challenges of isolating substantial numbers of mouse optic nerve OPCs, we examined whether rat OPCs could also myelinate mouse RGC axons (Figure 4B). We found that rat optic nerve OPCs differentiated and ensheathed mouse RGC axons robustly in the presence of DAPT (Figures 4D and 4F). Moreover, Sudan Black staining and EM revealed that rat cortical cells generate compact myelin around mouse axons (Figures 4G and 4H). These results provide evidence that mouse and rat neurons and glia may be used interchangeably in these cocultures in order to exploit the distinct advantages of each.

## During which Stages of Maturation can an Oligodendrocyte Myelinate?

We next explored whether the use of differentiated OLs might result in more rapid ensheathment of axons and enable experimental isolation of myelination from differentiation. We used cell surface markers to purify distinct stages of the OL lineage and evaluated their ability to ensheath RGC axons. Three stages were isolated in parallel from developing rat optic nerves: OL-depleted OPCs, OPC-depleted MOG<sup>+</sup> OLs, and an intermediate stage of GC-expressing 'immature OLs' that do not yet express MOG. Whereas OPCs readily developed into myelinating OLs in the presence of DAPT, mature OLs largely failed to ensheath RGC axons despite frequently extending MBP-rich processes (Figures 5A and 5B). Immature OLs also exhibited a substantial reduction in myelination compared to OLs that were newly generated from OPCs. Lineage progression, not simply aging, is important for this reduction in myelination, as purified adult OPCs readily develop into myelinating OLs (Figure 5C). These results suggest that maturation of OLs is associated with a rapid loss in the capacity to robustly initiate new myelin segments.

Is the inability of mature OLs to myelinate due to extrinsic factors, such as the presence of copurified myelin debris or the absence of nearby OPCs and astrocytes? To address this question, we utilized OPCs from the cortices of transgenic mice. We first confirmed that, similar to rat optic nerve cells, mouse cortical cells display a progressive loss in the ability to myelinate (Figures S2A and S2B). We then cocultured both transgenic GFP<sup>+</sup> OPCs and wild-type mature OLs side-by-side on the same RGC axons. Even as neighboring GFP<sup>+</sup> OPCs became myelinating OLs, mature OLs mostly failed to myelinate (Figures S2C and S2D). These results indicate that the loss in the ability to myelinate is intrinsic.

To further evaluate the timeframe within OL maturation for myelin initiation, we next adapted the coculture for time-lapse microscopy, utilizing a highly-efficient nucleofection technique for rat cortical OPCs (Dugas et al., 2006). Transfected OPCs expressing a farnesylated (*i.e.*, membrane-targeted) green fluorescent protein (EGFP-F) were imaged every ten minutes in the presence of DAPT. Figure 6A illustrates the typical pattern of myelin segment initiation (see also Movie S1). Six hours into imaging, this cell initiated multiple tubes of myelin, establishing as many as seven segments over the next twelve hours. The OL initiated no new stable segments over the following twelve hours, despite continued interactions between OL processes and axons. While we observed extensive segment remodeling, including extension and retraction, well-defined stable segments were rarely established after the initial period (Figures 6A, 6B, and Movie S2). These observations suggest that OLs generally initiate all of the myelin segments that they will form within a brief period.

In order to quantify the relative ability of newly formed OLs and more mature OLs to initiate new myelin segments, we imaged a number of EGFP-F-expressing cells once per day while monitoring a reporter of OL maturity. The MBP promoter drove the expression of a farnesylated red fluorescent protein (mCherry-F) such that red fluorescence increased sharply upon differentiation but leveled as the OL matured (Figure 6B). Among the 52 cells that clearly increased mCherry-F expression (*i.e.*, the newly formed OLs), 36 of them formed new myelin segments (Figure 6C). In contrast, among the 39 myelinating OLs that displayed near-maximal mCherry-F expression, only six added a new myelin segment. (All eight non-myelinating OLs with stably high mCherry-F also failed to initiate segments.) These data imply that myelination primarily occurs early in differentiation, and that mature OLs are relatively incapable of myelinating compared to newly formed OLs. We conclude that the program of terminal differentiation includes a brief window during which myelination occurs followed by a rapid intrinsic loss in the capacity to myelinate.

## What Aspects of Myelination are Affected by White Matter Astrocytes?

We next evaluated the utility of this coculture system for dissecting the roles of additional CNS cells in myelination. Recent studies have demonstrated that astrocytes promote CNS myelination in multiple culture models (Ishibashi et al., 2006; Sorensen et al., 2008). We exploited the ability to establish cocultures with minimal endogenous generation of astrocytes to explore which stages of myelination are affected by white matter astrocytes. Purified rat optic nerve astrocytes were plated onto RGC reaggregate cultures two days prior to seeding optic nerve OPCs. After six days of coculture in MyM, we examined cell fates and ensheathment of axons by immunostaining for MBP and MOG, as well as the degree of myelin wrapping by Sudan black (Figure 7). Analysis of cell fate markers revealed that astrocytes reduced OL differentiation, either in the presence or absence of DAPT, compared to the equivalent condition without astrocytes (Figure 7B). Evaluation of OL morphology showed that, unlike DAPT, astrocytes did not contribute substantially to the proportion of MOG<sup>+</sup> OLs that were ensheathing axons (Figure 7C). Despite the partial inhibition of differentiation and the lack of strong effects on ensheathment, Sudan Black staining indicated that astrocytes enhance both the numbers of OLs forming compact myelin (Figure 7D) and the qualitative appearance of myelinating cells (Figure 7E). To assess whether this difference represents a differentiation- and ensheathment-independent increase in wrapping, we normalized the numbers of myelinating OLs determined by Sudan Black with the numbers of ensheathing MOG<sup>+</sup> cells determined in companion cultures. Correcting for the numbers of ensheathing OLs under the various conditions, we found that astrocytes specifically enhance myelin thickness (Figure 7D). Accordingly, examination of DAPT-treated cocultures by EM revealed that the typical myelinated axon at 6 days had 2–4 wraps of compact myelin (Figure 7F). We observed thicker myelin in the presence of astrocytes (Figure 7F) or over an additional 3 days without astrocytes, including examples of mature multilamellar myelin and paranodal loops (Figures 7F and 7G). In other experiments, we found that the inclusion of optic nerve astrocytes enhanced the rate of wrapping in cortical OPC cocultures, with Sudan Black-labeled myelin segments evident by the fourth day (Figure S3). Together these results indicate that optic nerve astrocytes enhance the speed and degree of wrapping but are not essential for the generation of compact myelin. This coculture system therefore enables evaluation of the factors that directly influence wrapping and compaction and provides a valuable tool for scrutinizing the precise functions of defined populations of astrocytes or other CNS cells in myelination.

## Regulation of Myelination by Glial $\gamma$ -Secretase

Finally, we investigated the utility of this coculture system for dissecting molecular mechanisms of myelination, focusing on understanding the effects of  $\gamma$ -secretase inhibition on differentiation and ensheathment. In order to test whether these effects were due to the blockade of Notch1 signaling, we cultured Notch1-deficient OPCs with rat RGC reagggregates. Cortical OPCs from conditional Notch1 knockout mice (Radtke et al., 1999) were infected with a Cre recombinase adenovirus (AdCre) or a control virus (AdEmpty). Knockout of Notch1 was confirmed by  $\alpha$ -Notch1 immunostaining after three days of coculture (Figures 8A and 8B). At seven days, the knockout of Notch1 had increased the percentage of cells that express MBP by ~2-fold, but the majority of cortical OPCs still failed to become OLs (Figure 8C). Consistent with the modest differentiation effects of DAPT in rat cortical OPC cocultures, these results suggest that Notch1 activation contributes to the axonal blockade of cortical OL development but is not the only mediator of this inhibition.

Despite the increase in OL differentiation, Notch1 knockout did not affect the proportion of these MBP<sup>+</sup> cells that ensheathed RGC axons as they differentiated. We did, however, observe a significant enhancement in myelination when DAPT was added on the third day (Figures 8D and 8E). These findings suggest a previously unrecognized function of  $\gamma$ -secretase activity in

controlling OL myelination that is independent of its role in Notch1 activation and differentiation.

Both neurons and glia express the essential components of the  $\gamma$ -secretase complex (Cahoy et al., 2007), including the protease active site imparted by either presenilin-1 or presenilin-2 (Selkoe and Wolfe, 2007). To determine whether inhibition of  $\gamma$ -secretase specifically in OL-lineage cells is sufficient to mimic the effects of DAPT, we examined myelination of rat RGC axons by presenilin-deficient OLs. OPCs were acutely purified from transgenic mice that lack presenilin-2 and lose presenilin-1 upon Cre-mediated recombination (Saura et al., 2004). Infection of these OPCs with AdCre, like DAPT, significantly increases the percentage of OLs that ensheath axons (Figure 8F). Together, these results implicate glial  $\gamma$ -secretase in the regulation of myelination in at least two ways: in the control of differentiation by Notch1 signaling and in the Notch1-independent modulation of myelin segment initiation. Thus the current technique has enabled the molecular uncoupling of the roles of  $\gamma$ -secretase in differentiation and myelination.

## DISCUSSION

### Development and Utility of a Rapidly Myelinating CNS Coculture System

A detailed understanding of the regulation and mechanisms of CNS myelination will require integrating a variety of approaches, ranging from the glial cell culture to the targeted disruption of genes in transgenic mice. While no single technique will be sufficient, myelinating culture systems provide an important bridge between purified OPCs and complex *in vivo* approaches. Our CNS coculture closely reflects the composition of the optic nerve and provides a robust model system for understanding CNS myelination. As such, it provides the opportunity to generate hypotheses that can be tested *in vivo*, as well as to investigate mechanistically observations made in animal models.

This method offers a number of virtues that will make it a valuable tool for a variety of studies. First, the system relies on a unique architecture of defined cell populations, providing the extensive axon-glia contact characteristic of explant cultures while allowing for independent manipulations of neurons and glia. Second, this myelinating coculture is relatively rapid, with substantial numbers of OPCs differentiating and ensheathing RGC axons within four days of their isolation in the presence of  $\gamma$ -secretase inhibitors. Finally, acutely isolated OPCs manipulated by transient nucleofection or recombinant adenoviral infection rapidly myelinate RGC axons, enabling molecular dissection of multiple aspects of myelination. Recent gene profiling studies indicate that as OPCs differentiate into myelinating OLs, they are progressively marching through a genetic program that enables them first to migrate, then to adhere to axons, to myelinate, and finally to form the node and paranode (Cahoy et al., 2007; Dugas et al., 2006). These studies identified novel OL genes that are regulated during each of these steps. The current technique provides a defined system to genetically dissect these processes.

In addition to these features, this coculture can be adapted for use with cells from a range of sources. We show, for example, that OPCs isolated from either rat or mouse generate OLs that can myelinate either rat or mouse RGC axons. Moreover, this system enables the use of OL-lineage cells from different CNS regions and stages of development. It is likely that the current approach may also be generalizable for adapting other CNS neurons to myelinating cocultures, although this has not yet been established. Various neuronal populations differ substantially in their requirements for purification, differentiation, and axon growth, and the conditions for most CNS neurons are not yet optimized. When conditions are determined for particular neurons, features of the current technique, such as the use of reaggregates and  $\gamma$ -secretase inhibitors, may help to guide their application to myelination studies. In addition to these future

possibilities for diversifying neuronal populations, the current data illustrate the value of this system for investigating other defined cell types in myelination, revealing a specific role for optic nerve astrocytes in myelin growth. These various approaches indicate the versatility of this technique.

While this coculture offers a number of advantages, it may also require a greater effort to establish than some *in vitro* methods, such as mixed brain cultures, though not substantially more than DRG cocultures. Immunopanning techniques do not require special equipment, are robust, and are technically similar across a range of cell types. Combining cell purifications can reduce animal and labor costs. These technical considerations are also balanced by the reliability and adaptability of this system for analyzing factors influencing multiple stages of myelination. The utility of mixing genetically modified purified cell types may extend well beyond the development of myelin to mechanistic questions of demyelination, viral infection, and immune activation. This system may, for example, be adapted to investigate T cell activation by myelin epitopes, the astrocytic response to demyelination, or factors influencing the stability of myelin. Given these considerations, the investment in establishing this coculture will frequently be worth the opportunities it provides to address mechanistic questions in a defined setting.

### **Oligodendrocytes Myelinate Only during a Brief Time Window Early in their Differentiation**

The ability of mature OLs to form new myelin has long been a topic of investigation. Although early studies suggested that GC<sup>+</sup> cells isolated from adult rats generate myelin when transplanted into the brains of *shiverer* mice (Lubetzki et al., 1988), other experiments indicate little contribution of postmitotic OLs to remyelination (Crang et al., 1998). The source of the observed differences between the capacity of OPCs and OLs to myelinate cannot be easily identified in these adult transplantation and remyelination experiments. Possibilities include misidentification of adult OPCs as OLs, differences in the abilities of OPCs and OLs to migrate to naked axons, extrinsic changes related to a damaged environment, age-dependent alterations in the capacity to generate new myelin, or developmental changes related to progression of OLs through the lineage. The simplified coculture described here provided an opportunity to directly observe defined stages of the lineage and follow the innate capacity of OLs to myelinate as they mature.

Using both time-lapse microscopy and coculture with selected stages of the OL lineage, we found that OLs have only a brief period of time, early during differentiation, in which they typically initiate all of the myelin segments that they will form. Despite frequent extension of MBP<sup>+</sup> processes by immature and mature OLs, we found that only perinatal and adult OPCs developed into myelinating OLs at a high rate. The period for myelination is remarkably brief and early in OL maturation, with the ability to wrap axons being reduced by the time an OL has lost surface expression of OPC markers. These findings reveal that OLs undergo a rapid intrinsic loss of the capacity to myelinate as they mature. The coculture system should enable investigation of pharmacological and genetic approaches that may stimulate mature OLs to regain the ability to myelinate.

### **Inhibition of Glial $\gamma$ -Secretase Stimulates CNS Myelination**

Our findings add to the growing evidence that axonal signals play a critical role in controlling not only the timing of differentiation but also the initiation of myelination. Axonal Notch1 ligands, for instance, are likely to inhibit OPCs from prematurely differentiating. Conditional knockout mice in which the Notch1 gene is eliminated in the OL lineage exhibit premature and ectopic OL differentiation (Genoud et al., 2002). The generation of OLs at this early stage leads to OL apoptosis and early lethality, precluding examination of myelination. Thus the action of  $\gamma$ -secretase in OPC Notch1 signaling makes it difficult to dissect the role of  $\gamma$ -secretase



in newly generated OLs. By allowing for the uncoupling of myelination from OL differentiation and survival (Rosenberg et al., 2007), the RGC-OPC coculture system enabled investigation of the distinct roles of  $\gamma$ -secretase in OPCs and newly formed OLs. We found that, even when OL differentiation was promoted by Notch1 knockout, the proportion of OLs that myelinated during differentiation was significantly enhanced by  $\gamma$ -secretase inhibition. Glial  $\gamma$ -secretase therefore regulates myelination at two stages: it facilitates the inhibition of OPC differentiation by Notch1 activation, and it restricts myelination by differentiating OLs. These results provide evidence that there are molecularly distinct mechanisms, both involving  $\gamma$ -secretase, that regulate OL differentiation and the ensheathment of axons.

How does glial  $\gamma$ -secretase activity restrict myelination? Typically stimulated by an initial cleavage by another protease,  $\gamma$ -secretase acts on at least three dozen transmembrane substrates (Selkoe and Wolfe, 2007), some of which have been previously implicated in controlling glial development, such as neuregulin-1 (Michailov et al., 2004; Taveggia et al., 2005), erbB4 (Sussman et al., 2005), and N-cadherin (Schnadelbach et al., 2001). An interesting possibility consistent with our findings is that there may be an axonal signal that induces myelination by directly or indirectly inhibiting  $\gamma$ -secretase in OLs (see below). The identity and regulation of the relevant  $\gamma$ -secretase substrate are therefore important questions for future studies.

The inclusion of  $\gamma$ -secretase inhibitors to stimulate differentiation and ensheathment in these cocultures presumably rescues the need for signals provided in development but not adequately supplied *in vitro*. We expect that this system will be of value in deciphering these signals, so that more physiological means may be employed to achieve robust myelination. The use of these inhibitors, however, necessitates caution, as it is uncertain whether they might cause distortions to the normal myelination process. Importantly, these inhibitors are not required for differentiation and ensheathment, so they may be excluded as desired. Moreover,  $\gamma$ -secretase inhibition does not influence myelin wrapping or compaction. Thus later stages of myelination may best be studied with the addition of DAPT only during the first few days of coculture.

An important implication of our findings is that  $\gamma$ -secretase inhibitors may promote remyelination in demyelinating diseases. Inhibitors of  $\gamma$ -secretase have already been shown to reduce the severity of experimental autoimmune encephalomyelitis (EAE), a mouse model of MS. It has been suggested that these inhibitors relieve EAE by blocking Notch1 signaling in either T cells (Minter et al., 2005) or OPCs (Jurynczyk et al., 2005). Our finding that  $\gamma$ -secretase inhibition stimulates myelination independently of Notch1 suggests an additional mechanism by which these drugs may ameliorate EAE. The coculture system will be useful for identifying the molecular mechanism by which  $\gamma$ -secretase influences myelination and thus more specific targets to help promote remyelination.

### **Astrocytes Promote Myelin Wrapping and Compaction**

Astrocytes are increasingly recognized to contribute to CNS myelination (Sorensen et al., 2008). Astrocytes, for example, promote myelination in response to electrical activity by releasing the cytokine leukemia inhibitory factor (Ishibashi et al., 2006). In addition to signaling, astrocytes may support myelination in other ways, perhaps by coating axons with myelin-promoting extracellular matrix molecules, providing lipids for myelin synthesis, or modulating electrical activity. The RGC coculture system seems particularly well suited to elucidating the precise mechanisms by which astrocytes enhance myelination. This technique provides the ability to analyze and control distinct stages of myelination, to rapidly induce nearly complete OL differentiation with minimal endogenous astrocyte generation, and to provide anatomically appropriate white matter astrocytes. Using these advantages, we provide evidence that the predominant role of astrocytes is in promoting rapid myelin growth rather

than in enhancing the initiation of myelination. The coculture system should enable future studies of the molecular basis of this interaction.

### **A Model for CNS Myelination**

It has long been thought that the probability that an OL process will ensheath an axon is governed solely by local signaling events at sites of axon-glia contact. The CNS coculture system permits evaluation of this hypothesis, and our results suggest an alternative model. We found that an OL forms all of its myelin segments nearly concurrently during a transient period early in the process of differentiation. This coincident cell-wide initiation suggests that the regulation of myelination includes a component of global control in addition to the local interactions between independent OL processes and axons. A potential mechanism for such cell-wide regulation is offered by our finding that the inhibition of glial  $\gamma$ -secretase promotes myelination. Given that the intracellular domains of cleaved  $\gamma$ -secretase substrates often serve to regulate transcription, our findings imply the existence of a nuclear-controlled myelination program that is suppressed by  $\gamma$ -secretase activity. A global decision to myelinate may normally be triggered by a reduction in  $\gamma$ -secretase activity when a sufficient number of OL processes contact axons. This provisional model raises the unexpected possibility that contact of an OL process with an axon influences not only its own wrapping but also the initiation of myelination of other axons by the same OL. The unique features of this CNS myelinating coculture system will continue to provide valuable tools for exploring this and other models in future studies.

## **EXPERIMENTAL PROCEDURES**

A step-by-step protocol for the OPC-RGC coculture, including modifications for immunopanning other cell types, can be found online (Supplemental Material).

### **Establishment of reagggregates of purified RGCs**

RGCs were purified to >99.5% homogeneity from three litters of 5-day-old (P5) rat retinae by immunopanning as previously described (Meyer-Franke et al., 1995). Briefly, dissected retinae were digested with papain at 35 C. Following gentle trituration, cells were resuspended in a panning buffer containing insulin (5  $\mu$ g/ml) and then incubated with rabbit  $\alpha$ -macrophage antibodies. Retinal cells were incubated sequentially on three immunopanning dishes: two coated with  $\alpha$ -rabbit secondary antibodies and the third with T11D7  $\alpha$ -Thy1 mAb. RGCs were released from the final panning dish with trypsin (Sigma). For mouse RGCs, the negative selection against macrophages was achieved using BSL I and positive selection with Serotec mouse  $\alpha$ -mouse Thy1.2 (see Supplemental Material).

To produce reagggregates, RGCs were plated at high density (>1,000 cells/ $\mu$ l) in 500  $\mu$ l ND-G medium (see Supplemental Material) in an 8-well chamber-slide (Nunc). After two days, reagggregates were collected, washed, and distributed on PDL-laminin-coated glass coverslips. Typically, ~2.2 million RGCs from 3 litters of rat pups or 6 litters of mouse pups were distributed as reagggregates over 24 coverslips. The following day, 450  $\mu$ l medium was added to each well.

### **Purification of optic nerve OPCs and maintenance of cocultures**

OPCs were purified to >99.5% homogeneity from 7- to 8-day-old (P7-P8) rat optic nerves by immunopanning as previously described (Barres et al., 1994). Briefly, optic nerves from 2–4 litters of rat pups were digested with papain at 35 C. Following gentle trituration, cells were incubated sequentially on three immunopanning dishes: Ran-2,  $\alpha$ -GC, and A2B5. OPCs were released from the final panning dish with trypsin and seeded onto established RGC reaggregate cultures at a density of 20,000 OPCs per well in ND-G or MyM medium, as indicated (see Supplemental Material). The  $\gamma$ -secretase inhibitor N-[N-(3,5-difluorophenacetyl)-L-alanyl]-S-

phenylglycine t-butyl ester (DAPT, Calbiochem, 5 mM in DMSO) was added to a final concentration of 1  $\mu$ M. Cocultures were maintained with  $\frac{1}{2}$  volume fresh medium changed every three days.

Mouse optic nerve OPCs were isolated from 5 litters of P7 mice (C57Bl6) by immunopanning using rat  $\alpha$ -mouse PDGFR $\alpha$  following a negative selection with BSL I (see Supplemental Material).

### Purification and transfection of rat cortical OPCs

OPCs were purified to >99.5% homogeneity from 7- to 8-day-old (P7–P8) rat brain cortices by immunopanning as previously described (Dugas et al., 2006). Briefly, cerebral hemispheres were diced and digested with papain at 37 C. Following gentle trituration, cells were incubated at room temperature sequentially on three immunopanning dishes: Ran-2,  $\alpha$ -GC, and O4. OPCs were released from the final panning dish with trypsin (Sigma).

For transfection, at least 1.5 million OPCs were plated on a 10-cm PDL-coated dish in ND-G medium for 2 hours to allow for recovery from the isolation. OPCs were then lifted off the dish by treatment with a 1:10 dilution of Trypsin-EDTA (Gibco), collected in 20% fetal calf serum, and resuspended in 100  $\mu$ l rat oligodendrocyte nucleofector solution (amaxa) containing 2  $\mu$ g plasmid. We performed nucleofection using amaxa program O-17 and seeded OPCs onto 2-week RGC reaggregate cultures at 180,000 cells per MatTek dish in ND-G containing 1  $\mu$ M DAPT.

pEGFP-F (Clontech) is a plasmid that encodes for a membrane-targeted form (*i.e.*, C-terminal farnesylation and palmitoylation sequences from c-Ha-Ras) of the enhanced green fluorescent protein under the control of the CMV promoter. mCherry cDNA, encoding for a monomeric variant of the red fluorescent protein DsRed (Shaner et al., 2004), was a gift from B. Baker (Stanford University) with the permission of R. Tsien (University of California-San Diego). To create a plasmid encoding for a membrane-targeted form of mCherry under the control of the MBP promoter (MBPp-mCherry-F), a PCR product containing mCherry was inserted in place of EGFP in pEGFP-F using standard techniques (Qiagen). The resulting mCherry-F gene was subcloned via NotI digestion into pMG2, a plasmid containing a 2-kb portion of the murine MBP promoter (Gow et al., 1992).

### Time-lapse microscopy

Rat cortical OPCs were cotransfected with plasmids encoding membrane-targeted fluorescent proteins (EGFP-F and mCherry-F) under the control of constitutive (CMV) and OL-specific (MBPp) promoters. Cotransfected OPCs were seeded onto established RGC reaggregate cultures grown on PDL- and laminin-coated glass-bottomed imaging dishes (MatTek). Following 3–4 days of coculture, OPCs amongst dense RGC axons were identified by light microscopy. Dual-color images of these cells were collected with a Cascade:1K CCD camera every ten minutes or once per day as indicated in a temperature ( $36\pm 1$  C) and CO<sub>2</sub>(10%)-controlled Nikon inverted epifluorescence microscope chamber, using an automated stage (Prior) under the control of Metamorph 2.0 software. To evaluate OL maturation and myelination, OPCs expressing EGFP-F were tracked daily beginning on the third or fourth day for expression of mCherry-F and initiation of new myelin segments. Periods during which mCherry-F markedly increased expression (>2-fold) from a low level were grouped as “differentiating” (*i.e.*, immature) OLs, whereas periods during which relatively high mCherry-F expression changed only modestly (*i.e.*, near-maximal) were defined as mature OLs. The majority of tracked OPCs failed to express mCherry-F at any point, and these were therefore excluded from the analysis.

### Conditional knockout cells & infection with AdCre

Presenilin double conditional knockout mice ( $PS1^{flox/flox}PS2^{-/-}$ ) (Saura et al., 2004) were a gift from Jie Shen (Brigham and Women's Hospital). Notch1 conditional knockout mice ( $Notch1^{flox/flox}$ ) (Radtke et al., 1999) were generously provided by Genentech. OPCs were purified from the cortices of P9 transgenic mice by immunopanning as described previously (Chan et al., 2004). Acutely-purified OPCs were infected at a multiplicity of infection of 10 for three hours with replication-defective AdEmpty or AdCre (University of Iowa Gene Transfer Vector Core), prior to passaging at 80,000 cells per well onto RGC reaggregate cultures. DAPT was added to a final concentration of 1  $\mu$ M after three days.

### Purification of adult OPCs, immature OLs, and mature OLs

Adult OPCs were purified from the optic nerves of P30 rats by immunopanning as previously described (Shi et al., 1998). OPCs, immature OLs, and mature OLs were purified in parallel from 3 litters of P13 rats. Following digestion and trituration, one-third of the cells were subjected to standard OPC immunopanning ( $Ran-2^{-}$ ,  $GC^{-}$ ,  $A2B5^{+}$ ). The remaining cells were incubated sequentially at room temperature on the following panning dishes:  $Ran-2$ ,  $A2B5$ , and  $\alpha$ -MOG (clone 8-18C5). Mature  $MOG^{+} A2B5^{-}$  OLs were released from the  $\alpha$ -MOG dish by trypsin (Sigma), while the remaining cells were incubated on a final  $\alpha$ -GC dish to isolate immature  $GC^{+} MOG^{-} A2B5^{-}$  OLs.

Purification of identified stages of OL-lineage cells from eight P13 mouse brains was performed as previously described (Cahoy et al., 2007). To isolate  $O4^{+} GC^{-}$  OPCs, cells were immunopanned using mouse  $\alpha$ -mouse Thy1.2,  $\alpha$ -GC, and O4. To isolate immature and mature OLs, dissociated cells were subjected sequentially to the following immunopanning dishes: BSLI lectin (x2), rat  $\alpha$ -mouse PDGFR $\alpha$ ,  $A2B5$ ,  $\alpha$ -MOG (x2), and  $\alpha$ -GC.  $MOG^{+} PDGFR\alpha^{-}$  mature OLs were released from the first MOG panning dish by trypsin.  $GC^{+} MOG^{-} PDGFR\alpha^{-}$  immature OLs were collected from final panning dish. Similar protocols were used to isolate OPCs from P5 transgenic mice ubiquitously expressing EGFP (Jackson Labs) in parallel with immature and mature OLs from P13 wild-type mice (C57Bl6).

### Purification of optic nerve astrocytes

White matter astrocytes were purified from 3–4 litters of P2 rat optic nerves as previously described (Mi and Barres, 1999). Briefly, optic nerves were dissected and dissociated as for OPCs and passed over three immunopanning dishes: OX7  $\alpha$ -Thy1,  $A2B5$ , and C5. Astrocytes collected from the C5 dish were plated onto 1- to 2-week RGC reaggregate cultures 1–2 days prior to seeding of OPCs by removal of 300  $\mu$ l of medium and the addition of 500  $\mu$ l MyM containing 20,000–40,000 astrocytes per well.

### Immunostaining and quantification

Immunostaining of cocultures was performed as previously described (Chan et al., 2004) with one additional drying step. Briefly, cocultures were gently fixed with 4% PFA for 10 min, rinsed with phosphate-buffered saline (PBS), and air-dried 30 min. Cocultures were blocked with 50% normal goat serum (NGS) in an antibody buffer containing 0.4% Triton X-100. Primary antibodies were added either overnight at 4 C or for 90 min at room temperature in a buffer containing 10% NGS and 0.08% Triton. Incubation with Alexa 488-, Alexa 594-, and/or Alexa 680-labeled secondary antibodies (1:1000, Molecular Probes) for 45 min was followed by rinsing and mounting on slides using Vectashield with DAPI.

Primary antibodies used in this study included: rabbit  $\alpha$ -NG2 (Chemicon), mouse  $\alpha$ -MBP (Chemicon), rat  $\alpha$ -MBP (Abcam), mouse  $\alpha$ -CNP (Chemicon), chicken  $\alpha$ -PLP (Chemicon), mouse  $\alpha$ -GFAP (Sigma), mouse  $\alpha$ -pan-sodium channel (gift from J. Trimmer), rabbit  $\alpha$ -Caspr

(gift from E. Peles), mouse  $\alpha$ -MOG (clone 8-18C5, gift from M. Gardinier), goat  $\alpha$ -Notch1 (R&D Systems), mouse  $\alpha$ -Tau-1 (Boehringer Mannheim), SMI31  $\alpha$ -neurofilament heavy-chain (phosphorylated) (Sternberger Monoclonals), and mouse  $\alpha$ -MAP2 (Sigma).

For quantification, stained coverslips were blinded and images of 10 fields (20x objective) near reagggregates per coverslip were acquired on a Nikon epifluorescence microscope. Images were randomized and scored blindly for cell fate and, in the case of MBP<sup>+</sup> OLs, whether or not they were associated with multiple distinct, smooth tubes of myelin. All error bars are  $\pm$ SEM.

### Staining for Compact Myelin

Staining with Sudan Black B (Sigma) was performed as previously described (Ishibashi et al., 2006). Cocultures were fixed with 4% PFA for 10 min at room temperature, rinsed with PBS, and air-dried for 30 min. Following rehydration with PBS, cultures were postfixed for 1 hr with 1% OsO<sub>4</sub> in phosphate buffer. After 2 washes with water, the cultures were dehydrated with an ethanol series (25%, 50%, 70%) for 10 min each and incubated for 2 hr in a filtered 0.5% Sudan Black solution in 70% ethanol. Following a quick rinse with 70% ethanol, the cultures were washed once with 3% ethanol and rehydrated in PBS. Cultures were mounted using Glycergel (DAKO) and viewed by brightfield microscopy.

For dual-labeling of mature myelin with  $\alpha$ -MOG and FluoroMyelin Red (Invitrogen), cocultures were fixed with 4% PFA for 10 min, rinsed with PBS, and air-dried for 30 min. Cocultures were blocked for 20 min in 50% NGS, incubated for 1 hr with  $\alpha$ -MOG supernatant (1:20), rinsed with PBS, and incubated for 30 min with Alexa 488-conjugated goat  $\alpha$ -mouse antibodies (Invitrogen, 1:1000). After rinsing with PBS, compact myelin was stained with FluoroMyelin Red (1:300 in PBS) for 20 min and washed three times with PBS (10 min). Coverslips were mounted using Vectashield with DAPI.

### Electron microscopy

Electron microscopy was performed in conjunction with the Stanford Microbiology and Immunology Electron Microscopy Facility and Cell Sciences Imaging Facility. Cocultures were fixed in 2% glutaraldehyde/4% paraformaldehyde in sodium cacodylate buffer. Following treatment with 1% osmium tetroxide and 1% uranyl acetate, samples were embedded in epon. Sections were taken between 75–90 nm, picked up on formvar/carbon coated 75 mesh Cu grids, stained for 20 seconds in 1:1 super-saturated uranyl acetate in acetone followed by staining in 0.2% lead citrate. Images were acquired with the JEOL 1230 TEM at 80kV.

### Supplementary Material

Refer to Web version on PubMed Central for supplementary material.

### Acknowledgements

The authors thank ChunZhao Zhang for technical assistance in the preparation of cocultures. We are indebted to Nafisa Ghorri for processing cocultures for EM and Sudan Black and John Perrino and Lydia Joubert for assistance with EM image acquisition. This work was funded by the National Eye Institute (R01 EY10257, BAB) and the Myelin Repair Foundation. B.E. is supported by an Australian NHMRC CJ Martin award.

### References

Barres BA, Lazar MA, Raff MC. A novel role for thyroid hormone, glucocorticoids and retinoic acid in timing oligodendrocyte development. *Development* 1994;120:1097–1108. [PubMed: 8026323]

- Bunge RP. Tissue culture observations relevant to the study of axon-Schwann cell interactions during peripheral nerve development and repair. *J Exp Biol* 1987;132:21–34. [PubMed: 3323401]
- Cahoy JD, Emery B, Kaushal A, Foo LC, Zamanian JL, Christopherson KS, Xing Y, Lubischer JL, Krieg P, Krupenko SA, et al. A Transcriptome Database for Astrocytes, Neurons, and Oligodendrocytes: A New Resource for Understanding Brain Development and Function. *J Neurosci* 2007;28:264–278. [PubMed: 18171944]
- Chan JR, Watkins TA, Cosgaya JM, Zhang C, Chen L, Reichardt LF, Shooter EM, Barres BA. NGF controls axonal receptivity to myelination by Schwann cells or oligodendrocytes. *Neuron* 2004;43:183–191. [PubMed: 15260955]
- Crang AJ, Gilson J, Blakemore WF. The demonstration by transplantation of the very restricted remyelinating potential of post-mitotic oligodendrocytes. *J Neurocytol* 1998;27:541–553. [PubMed: 11246493]
- De Strooper B, Annaert W, Cupers P, Saftig P, Craessaerts K, Mumm JS, Schroeter EH, Schrijvers V, Wolfe MS, Ray WJ, et al. A presenilin-1-dependent gamma-secretase-like protease mediates release of Notch intracellular domain. *Nature* 1999;398:518–522. [PubMed: 10206645]
- Dovey HF, John V, Anderson JP, Chen LZ, de Saint Andrieu P, Fang LY, Freedman SB, Folmer B, Goldbach E, Holsztynska EJ, et al. Functional gamma-secretase inhibitors reduce beta-amyloid peptide levels in brain. *J Neurochem* 2001;76:173–181. [PubMed: 11145990]
- Dugas JC, Tai YC, Speed TP, Ngai J, Barres BA. Functional genomic analysis of oligodendrocyte differentiation. *J Neurosci* 2006;26:10967–10983. [PubMed: 17065439]
- Genoud S, Lappe-Siefke C, Goebbels S, Radtke F, Aguet M, Scherer SS, Suter U, Nave KA, Mantei N. Notch1 control of oligodendrocyte differentiation in the spinal cord. *J Cell Biol* 2002;158:709–718. [PubMed: 12186854]
- Gow A, Friedrich VL Jr, Lazzarini RA. Myelin basic protein gene contains separate enhancers for oligodendrocyte and Schwann cell expression. *J Cell Biol* 1992;119:605–616. [PubMed: 1383235]
- Ishibashi T, Dakin KA, Stevens B, Lee PR, Kozlov SV, Stewart CL, Fields RD. Astrocytes promote myelination in response to electrical impulses. *Neuron* 2006;49:823–832. [PubMed: 16543131]
- Jurynczyk M, Jurewicz A, Bielecki B, Raine CS, Selmaj K. Inhibition of Notch signaling enhances tissue repair in an animal model of multiple sclerosis. *J Neuroimmunol* 2005;170:3–10. [PubMed: 16290267]
- Lubetzki C, Demerens C, Anglade P, Villarroya H, Frankfurter A, Lee VM, Zalc B. Even in culture, oligodendrocytes myelinate solely axons. *Proc Natl Acad Sci U S A* 1993;90:6820–6824. [PubMed: 8341704]
- Lubetzki C, Gansmuller A, Lachapelle F, Lombrail P, Gumpel M. Myelination by oligodendrocytes isolated from 4–6-week-old rat central nervous system and transplanted into newborn shiverer brain. *J Neurol Sci* 1988;88:161–175. [PubMed: 2465389]
- Meyer-Franke A, Kaplan MR, Pfrieger FW, Barres BA. Characterization of the signaling interactions that promote the survival and growth of developing retinal ganglion cells in culture. *Neuron* 1995;15:805–819. [PubMed: 7576630]
- Meyer-Franke A, Shen S, Barres BA. Astrocytes induce oligodendrocyte processes to align with and adhere to axons. *Mol Cell Neurosci* 1999;14:385–397. [PubMed: 10588392]
- Mi H, Barres BA. Purification and characterization of astrocyte precursor cells in the developing rat optic nerve. *J Neurosci* 1999;19:1049–1061. [PubMed: 9920668]
- Michailov GV, Sereda MW, Brinkmann BG, Fischer TM, Haug B, Birchmeier C, Role L, Lai C, Schwab MH, Nave KA. Axonal neuregulin-1 regulates myelin sheath thickness. *Science* 2004;304:700–703. [PubMed: 15044753]
- Minter LM, Turley DM, Das P, Shin HM, Joshi I, Lawlor RG, Cho OH, Palaga T, Gottipati S, Telfer JC, et al. Inhibitors of gamma-secretase block in vivo and in vitro T helper type 1 polarization by preventing Notch upregulation of Tbx21. *Nat Immunol* 2005;6:680–688. [PubMed: 15991363]
- Notterpek LM, Bullock PN, Malek-Hedayat S, Fisher R, Rome LH. Myelination in cerebellar slice cultures: development of a system amenable to biochemical analysis. *J Neurosci Res* 1993;36:621–634. [PubMed: 7511701]

- Radtko F, Wilson A, Stark G, Bauer M, van Meerwijk J, MacDonald HR, Aguet M. Deficient T cell fate specification in mice with an induced inactivation of Notch1. *Immunity* 1999;10:547–558. [PubMed: 10367900]
- Rosenberg SS, Powell BL, Chan JR. Receiving mixed signals: uncoupling oligodendrocyte differentiation and myelination. *Cell Mol Life Sci.* 2007
- Saura CA, Choi SY, Beglopoulos V, Malkani S, Zhang D, Shankaranarayana Rao BS, Chattarji S, Kelleher RJ 3rd, Kandel ER, Duff K, et al. Loss of presenilin function causes impairments of memory and synaptic plasticity followed by age-dependent neurodegeneration. *Neuron* 2004;42:23–36. [PubMed: 15066262]
- Schnadelbach O, Ozen I, Blaschuk OW, Meyer RL, Fawcett JW. N-cadherin is involved in axon-oligodendrocyte contact and myelination. *Mol Cell Neurosci* 2001;17:1084–1093. [PubMed: 11414796]
- Selkoe DJ, Wolfe MS. Presenilin: running with scissors in the membrane. *Cell* 2007;131:215–221. [PubMed: 17956719]
- Shaner NC, Campbell RE, Steinbach PA, Giepmans BN, Palmer AE, Tsien RY. Improved monomeric red, orange and yellow fluorescent proteins derived from *Discosoma* sp. red fluorescent protein. *Nat Biotechnol* 2004;22:1567–1572. [PubMed: 15558047]
- Shi J, Marinovich A, Barres BA. Purification and characterization of adult oligodendrocyte precursor cells from the rat optic nerve. *J Neurosci* 1998;18:4627–4636. [PubMed: 9614237]
- Sorensen A, Moffat K, Thomson C, Barnett SC. Astrocytes, but not olfactory ensheathing cells or Schwann cells, promote myelination of CNS axons in vitro. *Glia* 2008;56:750–763. [PubMed: 18293402]
- Sussman CR, Vartanian T, Miller RH. The ErbB4 neuregulin receptor mediates suppression of oligodendrocyte maturation. *J Neurosci* 2005;25:5757–5762. [PubMed: 15958742]
- Svenningsen AF, Shan WS, Colman DR, Pedraza L. Rapid method for culturing embryonic neuron-glia cell cocultures. *J Neurosci Res* 2003;72:565–573. [PubMed: 12749021]
- Taveggia C, Zanazzi G, Petrylak A, Yano H, Rosenbluth J, Einheber S, Xu X, Esper RM, Loeb JA, Shrager P, et al. Neuregulin-1 type III determines the ensheathment fate of axons. *Neuron* 2005;47:681–694. [PubMed: 16129398]
- Thomson CE, Hunter AM, Griffiths IR, Edgar JM, McCulloch MC. Murine spinal cord explants: a model for evaluating axonal growth and myelination in vitro. *J Neurosci Res* 2006;84:1703–1715. [PubMed: 17075918]
- Wang S, Sdrulla AD, diSibio G, Bush G, Nofziger D, Hicks C, Weinmaster G, Barres BA. Notch receptor activation inhibits oligodendrocyte differentiation. *Neuron* 1998;21:63–75. [PubMed: 9697852]

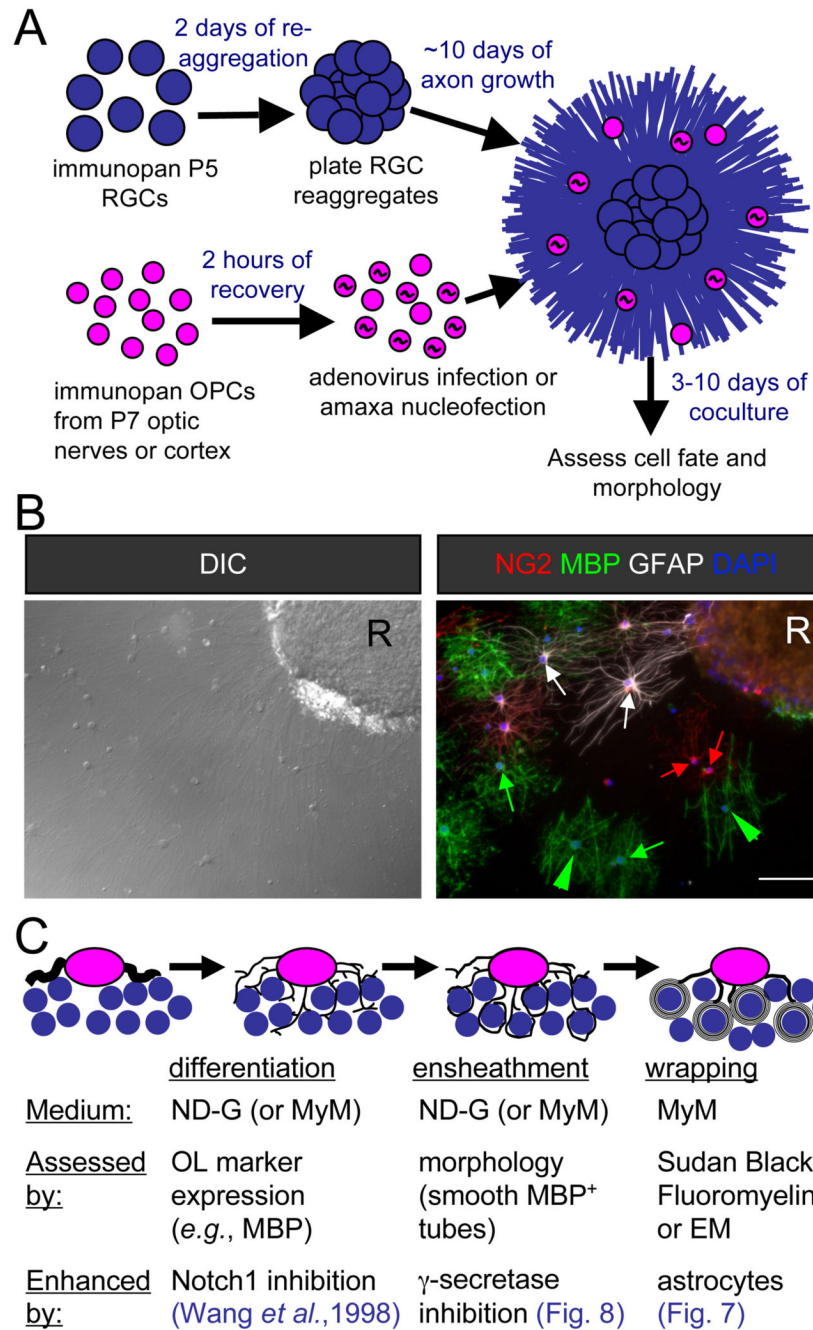


**Figure 1. Schematic of myelinating cocultures of OPCs with RGC reagggregates**

(A) Perinatal (P5) RGCs are purified by immunopanning and allowed to reaggregate for 2 days on a poorly-adhesive surface prior to plating on a substrate permissive for axon growth for 7–14 days. OPCs are then acutely isolated from optic nerves or cortices and, when transfection is necessary, recovered for a couple of hours to enable recombinant adenovirus infection or amaxa nucleofection. Transfer of these OPCs to the reaggregate cultures initiates the coculture that results in myelination, analyzed by immunostaining after six days.

(B) A coculture six days after seeding of optic nerve OPCs analyzed for cell fate and morphology by differential-interference contrast (DIC) microscopy and indirect immunofluorescence. Examples of OPCs (NG2, *red*), non-myelinating OLs (MBP, *green*), and



astrocytes (GFAP, *white*) are indicated by arrows of the corresponding colors. Myelinating OLs (*green arrowheads*) are identified by their extension of multiple distinctive smooth tubes. Nuclei are counterstained with DAPI (*blue*). An RGC reaggregate is denoted by “R”. Scale bar = 100  $\mu\text{m}$ .

(C) A schematic of the development of a myelinating OL in three stages. A bipolar OPC differentiates into an immature OL that begins to express myelin proteins and extends multiple processes amongst the RGC axons. These OL processes ensheath axons, depositing one smooth layer of membrane. The final stage consists of the wrapping of multiple layers of membrane and the extrusion of cytoplasm to form compact myelin.

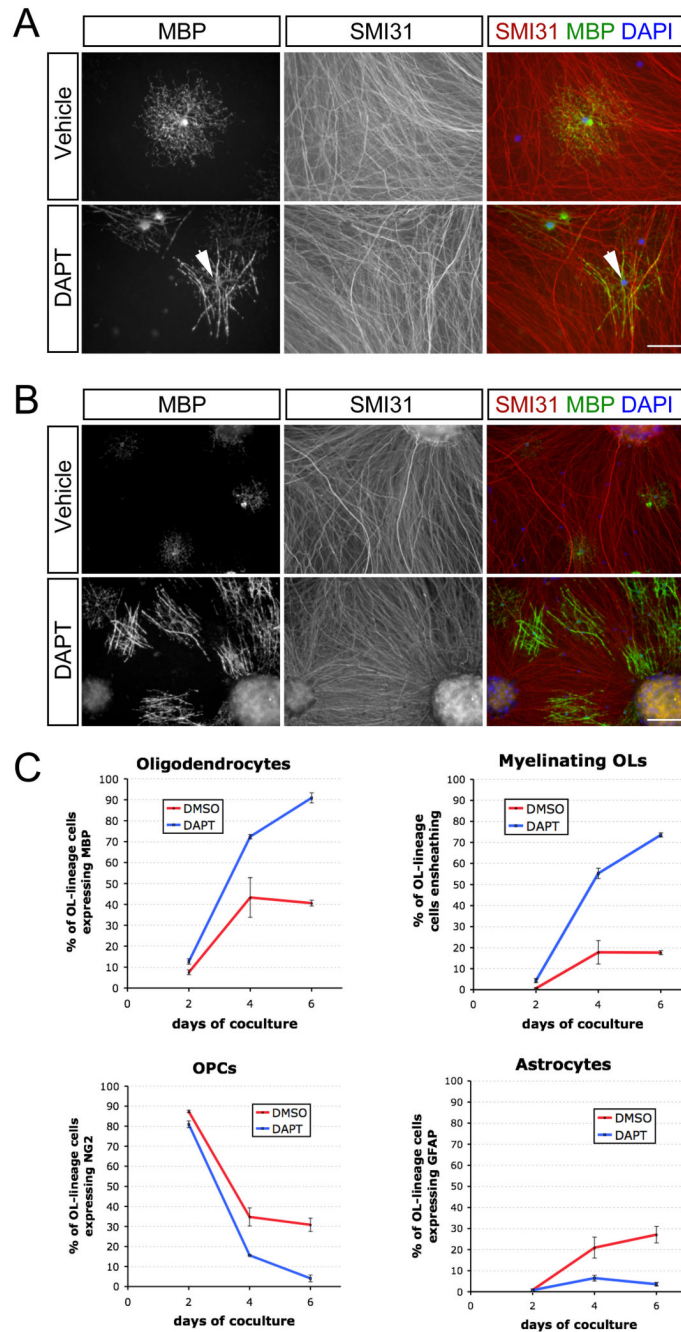


**Figure 2. Treatment of cocultures with a  $\gamma$ -secretase inhibitor disinhibits OL differentiation and myelination**

(A) Immunostaining of 3-day cocultures of optic nerve OPCs and RGC reagggregates treated with a  $\gamma$ -secretase inhibitor (1  $\mu$ M DAPT) or vehicle (DMSO) in ND-G medium. Early myelinating OLs (*arrowhead*) are observed after three days in the presence of DAPT. Scale bar = 50  $\mu$ m.

(B) Immunostaining of 4-day DAPT-treated cocultures reveals substantial OL differentiation and myelination. Scale bar = 100  $\mu$ m.

(C) Time-course of optic nerve OPC cell fates on RGC reagggregates in the presence (DAPT) or absence (DMSO) of a  $\gamma$ -secretase inhibitor ( $n = 3$  cocultures per condition).

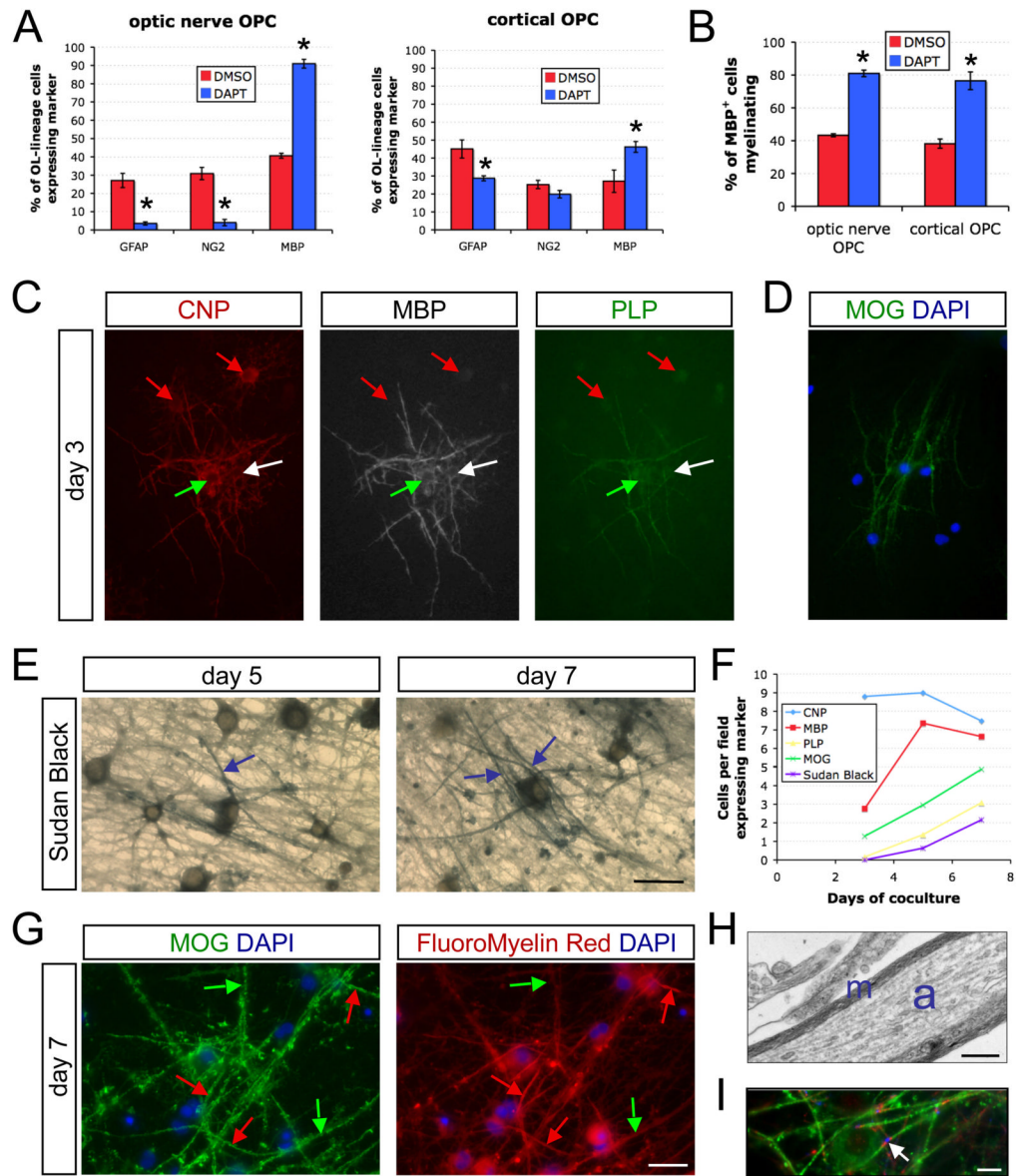


**Figure 3. Myelination in cocultures of cortical OPCs and RGC reagggregates**

(A) The disinhibition of differentiation upon  $\gamma$ -secretase inhibition (1  $\mu$ M DAPT) is less pronounced in RGC cocultures with cortical OPCs than in those with optic nerve OPCs after 6 days in ND-G (unpaired *t*-test,  $*p < 0.05$ ,  $n = 3$  cocultures per condition). Optic nerve OPC graph is replotted from day 6 data of Figure 3C. DMSO is the vehicle-only control.

(B) The proportion of MBP-expressing OLs forming myelin segments is equivalently enhanced by treatment with DAPT in both optic nerve and cortical OPC cocultures (unpaired *t*-test,  $*p < 0.005$ ,  $n = 3$  per condition).

(C) Triple labeling of cocultures grown for three days in MyM containing DAPT (1  $\mu$ M) reveals OLs in multiple stages of development. CNP<sup>+</sup> MBP<sup>-</sup> PLP<sup>-</sup> newly formed OLs (red arrows), CNP<sup>+</sup> MBP<sup>+</sup> PLP<sup>-</sup> immature OLs (white arrow), and CNP<sup>+</sup> MBP<sup>+</sup> PLP<sup>+</sup> myelinating OLs (green arrow) are observed at this stage. Scale bar = 50  $\mu$ m.

(D)  $\alpha$ -MOG immunostaining demonstrates isolated mature, ensheathing OLs on the third day of coculture. Scale bar = 50  $\mu$ m.

(E) Sudan Black staining of cocultures reveals thin compact myelin by day 5 with more advanced wrapping by day 7. Examples of Sudan Black-labeled myelin segments are indicated (*blue arrows*). Scale bar = 25  $\mu\text{m}$ .

(F) Time course of myelin markers in cocultures of rat cortical OPCs and rat RGCs over 7 days in MyM with DAPT, including sequential protein markers of OL maturation (CNP, MBP, PLP, and MOG) and a lipophilic dye reporting the degree of wrapping (Sudan Black). Numbers of cells displaying each marker was assessed over ten fields.

(G) Dual-labeling for OL maturation and ensheathment with  $\alpha$ -MOG and for compact myelin formation with the lipophilic dye FluoroMyelin-Red. Note that there are both myelinated segments (*red arrows*) and ensheathing or aligning OL processes that have not generated enough wraps to be detected above background (*green arrows*). Cell nuclei are counter-stained with DAPI. Scale bar = 25  $\mu\text{m}$ .

(H) Electron micrograph of a myelinated axon in a coculture of RGCs with cortical OPCs maintained for 7 days in MyM containing DAPT. The axon is indicated by the blue “a” and compact myelin by the blue “m”. Scale bar = 0.5  $\mu\text{m}$ .

(I) A node of Ranvier (*arrowhead*) in a 12-day DAPT-treated coculture in ND-G. A cluster of sodium channels (NaCh, *blue*) is flanked by clusters of a paranodal protein (Caspr, *red*) between the ends of two myelin sheaths (MBP, *green*). Scale bar = 10  $\mu\text{m}$ .

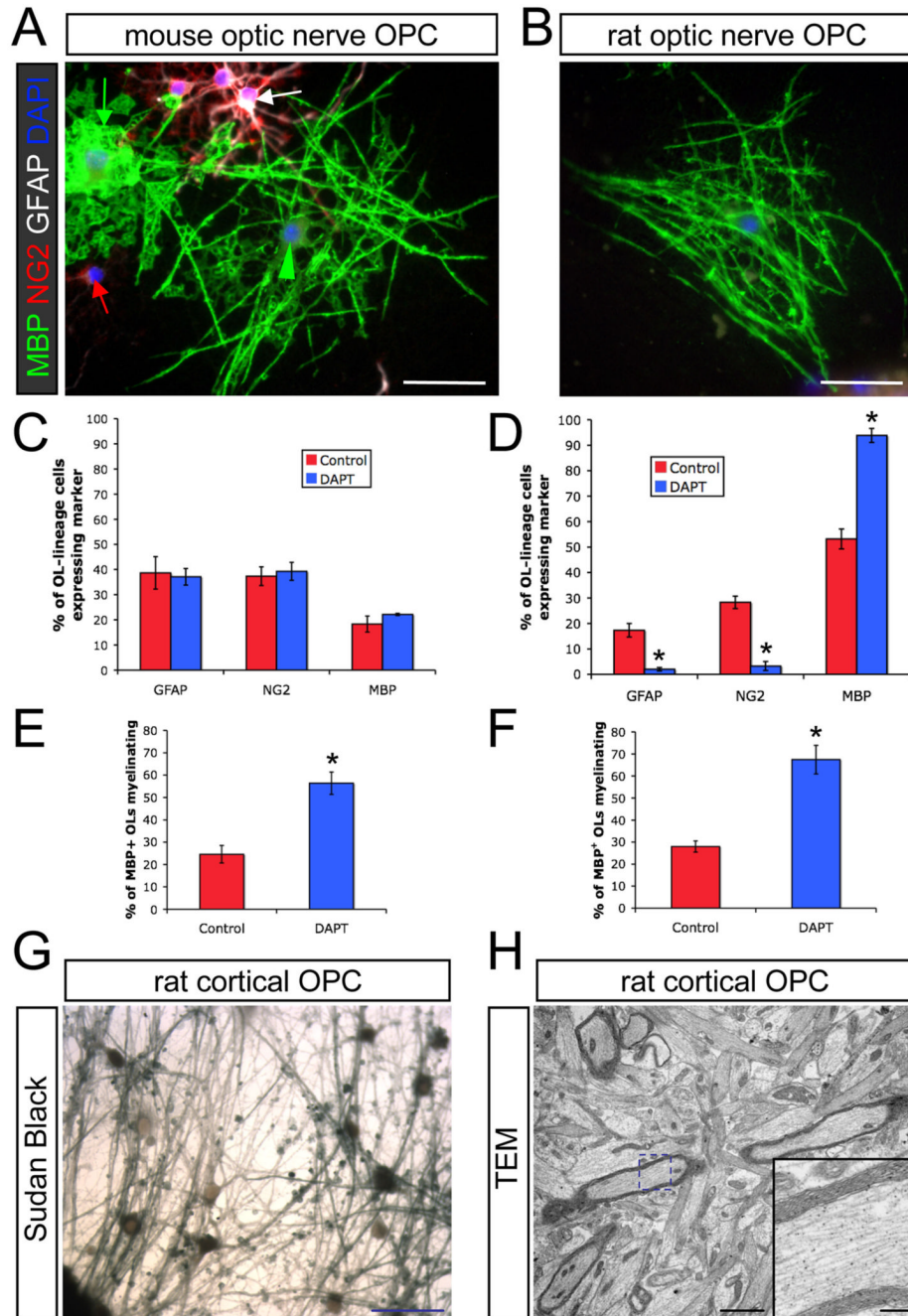


**Figure 4. Myelinating cocultures with mouse RGCs**

(A) Cocultures of mouse RGCs with mouse optic nerve OPC at day 6 in ND-G with DAPT (1  $\mu$ M) contain OPCs (red arrow), astrocytes (white arrow), non-myelinating OLs (green arrow), and myelinating OLs (green arrowhead). Scale bar = 50  $\mu$ m.

(B) An OL ensheathing RGC axons (MBP, green) in a coculture of rat optic nerve OPCs with mouse RGCs at day 6 in ND-G containing DAPT. Scale bar = 50  $\mu$ m.

(C) Coculture of mouse optic nerve OPCs with mouse RGCs results in significant inhibition of OL differentiation, even in the presence of DAPT ( $n = 4$  cocultures per condition).

(D) Inhibition of  $\gamma$ -secretase promotes nearly complete OL differentiation in cocultures of rat optic nerve OPCs with mouse RGCs (unpaired  $t$ -test,  $*p < 0.005$ ,  $n = 6$  cocultures per condition).

(E) Inhibition of  $\gamma$ -secretase with DAPT increases the proportion of mouse optic nerve OLs ensheathing mouse RGC axons (unpaired *t*-test,  $*p < 0.05$ ,  $n = 4$  cocultures per condition).

(F) Inhibition of  $\gamma$ -secretase with DAPT increases the proportion of rat optic nerve OLs ensheathing mouse RGC axons (unpaired *t*-test,  $*p < 0.005$ ,  $n = 6$  cocultures per condition).

(G) A DAPT-treated coculture of mouse RGCs and rat cortical OPCs stained for compact myelin with Sudan Black after 11 days of coculture (switched to MyM on day 5). Scale bar = 50  $\mu\text{m}$ .

(H) An electron micrograph of a companion coculture to the one seen in (G) shows multiple myelinated axons. Scale bar = 2  $\mu\text{m}$ . The blue dashed box indicates the region shown at higher magnification in the inset. Inset scale bar = 0.4  $\mu\text{m}$ .

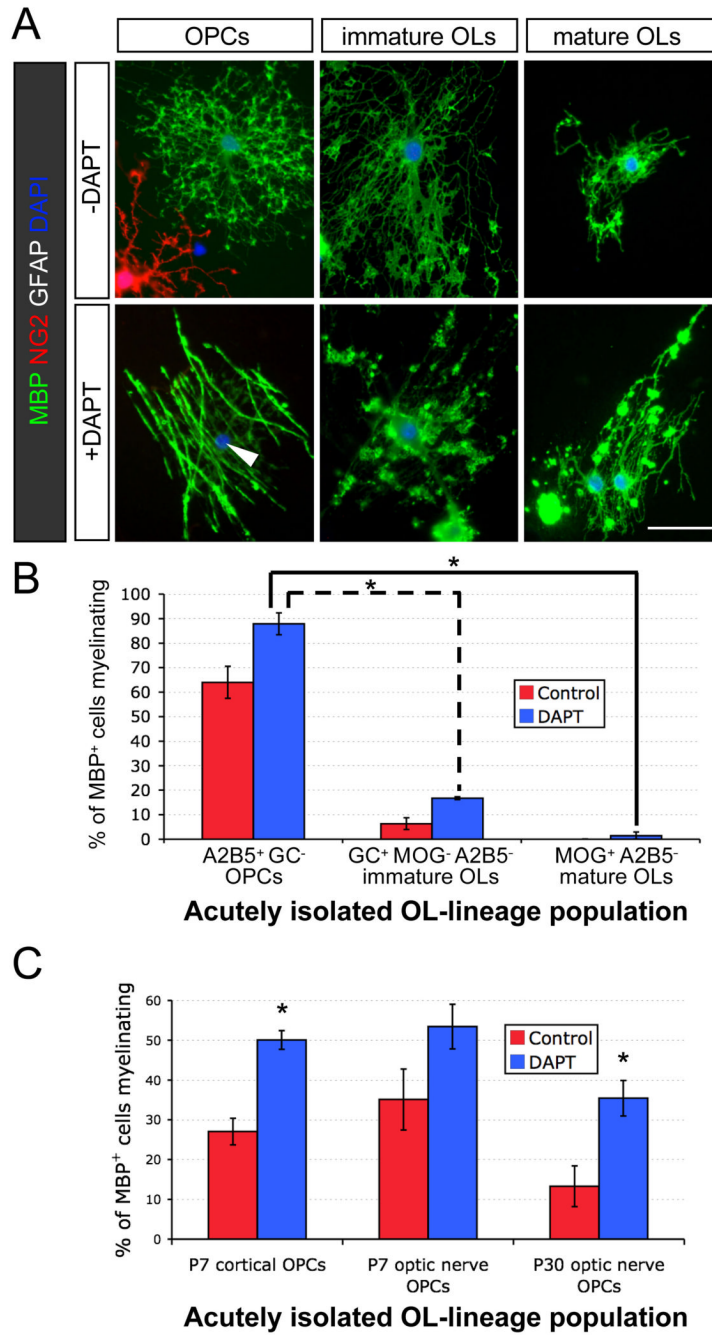


**Figure 5. Oligodendrocytes rapidly lose the capacity to myelinate as they progress through the lineage**

(A) Immunostaining of cocultures of RGCs with OPCs, immature OLs, or mature OLs that were acutely purified in parallel from P13 rat optic nerves. Cocultures were maintained in ND-G for six days in presence or absence of a  $\gamma$ -secretase inhibitor (1  $\mu$ M DAPT). Smooth myelin sheaths are extended by an OL that was newly generated from an OPC in the presence of DAPT (*arrowhead*), but the various morphologies of acutely isolated OLs rarely include distinct tubes of myelin around RGC axons. Scale bar = 50  $\mu$ m.

(B) OPC-depleted (A2B5<sup>-</sup>) populations of GC<sup>+</sup> and MOG<sup>+</sup> OLs from P13 rat optic nerves are limited in their ability to myelinate RGC axons (one-way ANOVA,  $p < 0.0001$ , post-hoc Tukey-Kramer tests,  $*p < 0.001$ ,  $n = 4$  per condition).

(C) Adult OPCs isolated from P30 rat optic nerves retain nearly the same capacity to develop into myelinating OLs as perinatal (P7) cortical or optic nerve OPCs (one-way ANOVA,  $p < 0.0001$ , post-hoc Tukey-Kramer tests,  $*p < 0.05$ ,  $n = 6-7$  per condition).



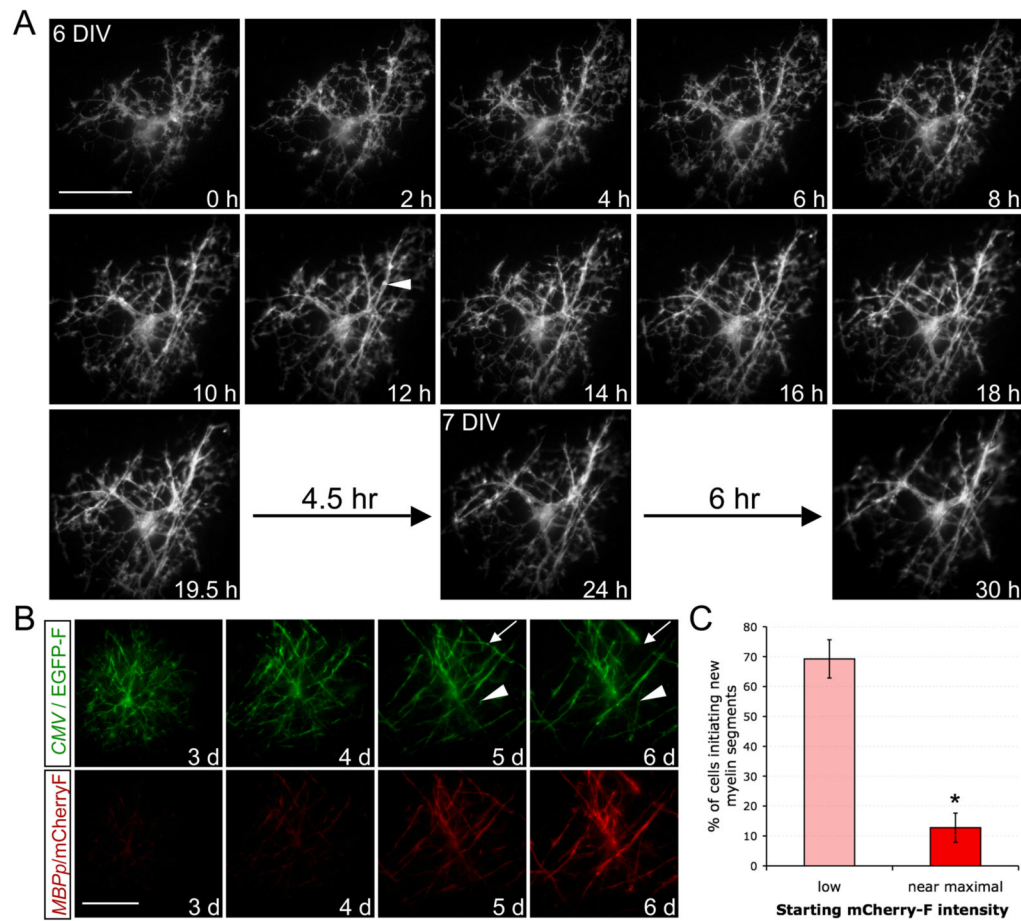


**Figure 6. Time-lapse microscopy reveals a brief window for myelination in the maturation of oligodendrocytes**

(A) Time-lapse of a developing OL expressing membrane-targeted EGFP-F as it initiated multiple myelin segments (*example indicated by arrowhead*) over a brief period (6h–18h), beginning during its sixth day *in vitro* (6 DIV) with RGC reagggregates in ND-G containing DAPT (1  $\mu$ M). Following this period, no new clear, stable segments were established (18h–30h). Scale bar = 50  $\mu$ m.

(B) Dual-color time-lapse of a developing OL expressing EGFP-F (*green*) under the control of the CMV promoter and mCherry-F (*red*) under the control of the MBP promoter (MBPp), beginning on the third day (3 d) of coculture in ND-G with DAPT. Multiple new myelin segments were initiated as mCherry-F expression increased, but days 5–6 were marked only by extension (*arrowhead*), retraction (*arrow*), and stabilization of existing segments, without formation of new ones. Scale bar = 50  $\mu$ m.

(C) Dual-transfected OPCs were evaluated for the initiation of new myelin segments and their expression of mCherry-F over 3–4 days. Mature OLs that began with near-maximal expression of mCherry-F rarely initiated new myelin segments, whereas newly differentiated OLs that clearly increased mCherry-F intensity frequently myelinated (% of cells forming at least one new clear myelin segment  $\pm$  standard error of the proportion,  $*p < 0.01$ ,  $z$ -test for independent proportions,  $n = 52$  cells that began with low or sub-maximal mCherry-F expression and 47 cells that began with near-maximal mCherry-F expression).

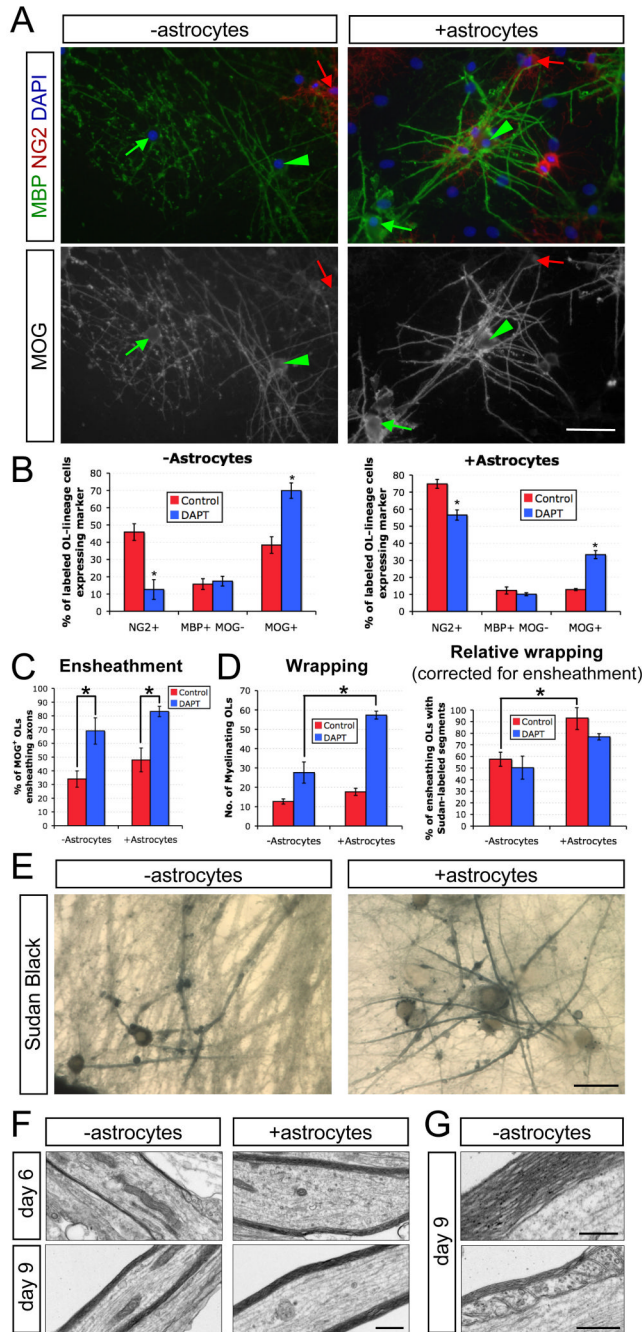


**Figure 7. Optic nerve astrocytes enhance the rate and degree of myelin wrapping in RGC-optic nerve OPC cocultures**

(A) Cocultures of rat RGCs and rat optic nerve OPCs with or without rat optic nerve astrocytes maintained for six days in MyM in the absence of DAPT. OPCs (NG2, red arrow), non-myelinating OLs (MBP, green arrow), and myelinating OLs (MBP, green arrowhead) can be detected by immunostaining. Scale bar = 50  $\mu$ m.

(B)  $\gamma$ -Secretase inhibition (1  $\mu$ M DAPT) increases differentiation of OLs from NG2<sup>+</sup> OPCs to MOG<sup>+</sup> OLs over six days of coculture in the presence or absence of optic nerve astrocytes (unpaired *t*-test, \**p*<0.005, *n* = 4 cocultures per condition).

(C)  $\gamma$ -Secretase inhibition (DAPT) promotes ensheathment of axons in the presence or absence of astrocytes, as assessed morphologically by the formation of two or more smooth tubes immunostained for MOG (one-way ANOVA,  $p < 0.005$ , post-hoc Tukey-Kramer tests,  $*p < 0.05$ ,  $n = 4$  per condition).

(D) Optic nerve astrocytes increase myelin thickness in cocultures, as determined by the total number of OLs forming Sudan Black-labeled myelin segments over ten 40x fields. A value corrected for the different number of OLs in each condition (Relative wrapping) was calculated by dividing this Sudan Black total by the average number of MOG<sup>+</sup> ensheathing OLs over the same area determined in companion cultures (one-way ANOVA,  $p < 0.05$ , post-hoc Tukey-Kramer tests,  $*p < 0.05$ ,  $n = 3$  per condition).

(E) Myelin wrapping is more advanced in cocultures containing optic nerve astrocytes, maintained for 6 days in MyM without DAPT, as seen by labeling with the lipophilic dye Sudan Black B. Scale bar = 25  $\mu\text{m}$ .

(F) Electron micrographs of 6- and 9-day cocultures of rat RGCs and rat optic nerve OPCs maintained in MyM with DAPT. Cocultures with added optic nerve astrocytes show more rapid and extensive wrapping of axons. Scale bar = 0.5  $\mu\text{m}$ .

(G) High-magnification electron micrographs of cocultures grown for 9 days in MyM with DAPT demonstrate that generation of thick myelin (*top image*) and mature paranodal loops (*bottom image*) occur even in the absence of added astrocytes over these longer culture periods. Scale bars = 0.2  $\mu\text{m}$  (*top*) and 0.5  $\mu\text{m}$  (*bottom*).

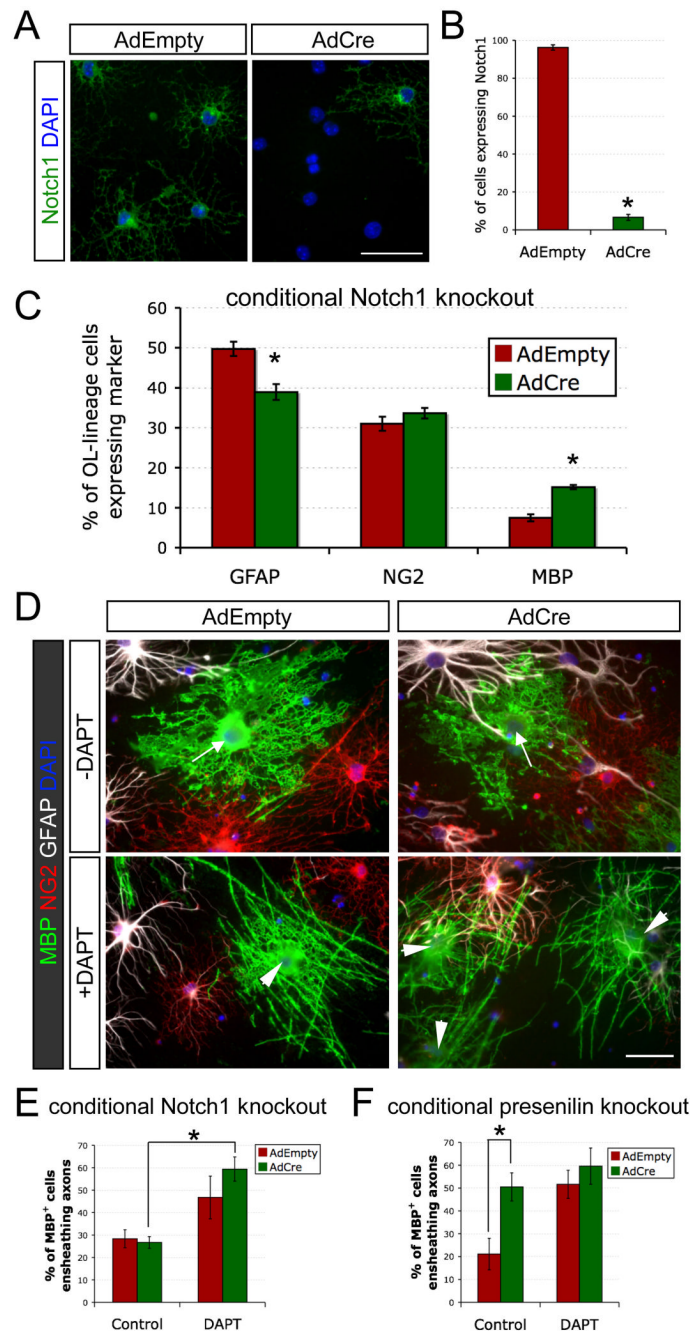


**Figure 8.  $\gamma$ -Secretase inhibition promotes ensheathment of RGC axons independently of Notch1**  
 (A) Cre-mediated knockout of glial Notch1 in cocultures. Acutely purified cortical OPCs from Notch1 conditional knockout mice were infected with a control replication-defective adenovirus (AdEmpty) or a recombinant adenovirus encoding Cre recombinase (AdCre) and cocultured for three days with rat RGC reagggregates prior to  $\alpha$ -Notch1 immunostaining (green). Cell nuclei were counterstained with DAPI (blue). Scale bar = 50  $\mu$ m.  
 (B) Quantification of AdCre-mediated Notch1 knockout at day 3 (percentage of live OL-lineage cells expressing Notch1  $\pm$  standard error of the proportion, \* $p$ <0.01, z-test for independent proportions,  $n$  = 186 cells for AdEmpty and 243 cells for AdCre).  
 (C) Quantification of the percentage of OL-lineage cells expressing markers (GFAP, NG2, MBP) in AdEmpty and AdCre treated cells.  
 (D) Fluorescence microscopy of MBP (green), NG2 (red), GFAP (red), and DAPI (blue) in AdEmpty and AdCre treated cells, with and without DAPT.  
 (E) Quantification of the percentage of MBP+ cells ensheathing axons in control and DAPT treated cells for conditional Notch1 knockout.  
 (F) Quantification of the percentage of MBP+ cells ensheathing axons in control and DAPT treated cells for conditional presenilin knockout.

(C) AdCre-mediated knockout of Notch1 increases OL differentiation over seven days in cocultures in ND-G (unpaired *t*-test,  $*p < 0.005$ ,  $n = 5$  per condition).

(D) Non-myelinating (*arrows*) and myelinating (*arrowheads*) OLs (*green*) in 7-day cocultures of RGCs with Notch1 conditional knockout OPCs. Immediately prior to seeding on RGC axons, acutely purified OPCs were infected for 2 hours with AdEmpty or AdCre. DAPT (1  $\mu\text{M}$ ) was added to the ND-G on the third day of coculture. Scale bar = 50  $\mu\text{m}$ .

(E) Addition of DAPT on the third day of coculture increases the proportion of OLs that form distinct myelin segments rather than sheets of MBP<sup>+</sup> membrane over seven days, independently of the presence (AdEmpty) or absence (AdCre) of Notch1 (one-way ANOVA,  $p < 0.005$ , post-hoc Tukey-Kramer test,  $*p < 0.01$ ,  $n = 5$  per condition).

(F) AdCre-mediated disruption of  $\gamma$ -secretase in presenilin-2-deficient, presenilin-1 conditional knockout OPCs promotes ensheathment of RGC axons equivalently to adding DAPT on the third day of coculture in ND-G (one-way ANOVA,  $p < 0.005$ , post-hoc Tukey-Kramer tests,  $*p < 0.05$ ,  $n = 5$ –6 per condition).